VIP Fluorescent Probes

DOI: 10.1002/anie.201102459

Synthesis and In Vivo Fate of Zwitterionic Near-Infrared Fluorophores**

Hak Soo Choi, Khaled Nasr, Sergey Alyabyev, Dina Feith, Jeong Heon Lee, Soon Hee Kim, Yoshitomo Ashitate, Hoon Hyun, Gabor Patonay, Lucjan Strekowski, Maged Henary, and John V. Frangioni**

A longstanding problem in the field of image-guided surgery is the development of ideal near-infrared (NIR) fluorophores. The heptamethine NIR fluorophore indocyanine green (ICG) has been used extensively for image-guided surgery because of its clinical availability and safety.[1–3] However, ICG is far from ideal because it exhibits high uptake in the liver, contaminates the gastrointestinal (GI) tract, provides moderate optical properties,[4] is unstable in aqueous media,[3,5] and is unable to conjugate covalently to targeting ligands.[2] Although several classes of novel molecules have been described,[6–13] none to date exhibit simultaneous low background binding, bifunctionality, excellent optical properties, low protein binding, and high serum stability. Although it is intuitive that physicochemical properties, that is, positive/negative charge density, hydrophilicity/lipophilicity, and charge distribution, will impact in vivo performance, chemical structures that exhibit ideal characteristics have not yet been defined.

[*] Dr. H. S. Choi, Dr. K. Nasr, D. Feith, J. H. Lee, Dr. S. H. Kim, Y. Ashitate, Dr. H. Hyun, Dr. J. V. Frangioni
Division of Hematology/Oncology, Department of Medicine and Department of Radiology, Beth Israel Deaconess Medical Center
330 Brookline Avenue, SLB-05, Boston, MA 02215 (USA)
Fax: (+1) 617-667-0981
E-mail: jfrangio@bidmc.harvard.edu

Dr. S. Alyabyev, Dr. G. Patonay, Dr. L. Strekowski, Dr. M. Henary
Department of Chemistry, Georgia State University
Atlanta, GA 30303 (USA)
Fax: (+1) 404-413-5505
E-mail: chemmh@langate.gsu.edu

Dr. S. H. Kim
WCU Department of BIN Fusion Technology
Chonbuk National University, Jeonju 561-756 (South Korea)

[**] This study was supported by the following grants from the National Institutes of Health: NCI BRP grant R01-CA-115296 (J.V.F.), NIBIB grant R01-EB-010022 (J.V.F. and H.S.C.), and NIBIB grant R01-EB-011523 (H.S.C. and J.V.F.). We thank Lindsey Gendall and Lorissa A. Moffitt for proofreading, and Linda Keys and Eugenia Trabucchi for administrative assistance. All FLARE technology is owned by Beth Israel Deaconess Medical Center, a teaching hospital of Harvard Medical School. As inventor, J. V. Frangioni may someday receive royalties if products are commercialized. J. V. Frangioni is the founder and unpaid director of The FLARE Foundation, a nonprofit organization focused on promoting the dissemination of medical imaging technology for research and clinical use.

Supporting information for this article is available on the WWW under http://dx.doi.org/10.1002/anie.201102459.

Previously, our group showed that rigid spherical nanoparticles, such as quantum dots, with a hydrodynamic diameter (HD) ≤ 5.5 nm could be rapidly cleared by the kidneys, and exhibit low background binding to normal tissues and organs, but only when the surface charge was neutral, geometrically balanced, and polyionic (referred to herein as zwitterionic for simplicity).[14–19] In this study, we explored the hypothesis that NIR fluorescent small molecules would exhibit improved in vitro and in vivo performance if synthesized with zwitterionic charges that are evenly spaced over the molecule to shield the underlying hydrophobicity of the relatively large heptamethine core.

We describe two complementary molecules, termed ZW800 $\pm i$ where $\pm i$ is the charge of the conjugated targeting ligand that will render the final molecule with a net charge of zero (i.e., zwitterionic). ZW800-1 has a net charge = 0 prior to targeting ligand conjugation, and a net charge = 0 after conjugation to a targeting ligand that has a net charge of -1 (that is, a targeting ligand with a net charge of 0 prior to conjugation). ZW800-3a has a net charge = $+2$ prior to conjugation, and a net charge = 0 after conjugation to a targeting ligand that has a net charge of -3 (that is, a targeting ligand with a net charge of -2 prior to conjugation). ZW800-1 and ZW800-3a were engineered for high hydrophilicity, with log$D$ (distribution coefficient) at pH 7.4 of -3.56 and -6.95, respectively. Importantly, these molecules have also been engineered with sulfonate groups to impart negative charge and quaternary ammonium cations (quats) to impart positive charge because preliminary results showed that the weaker, more common natural analogues (carboxylic acids and primary amines, respectively) did not exhibit the desired properties.

As depicted in Figure 1a, chloro-substituted NIR fluorophores **8** and **9** were synthesized by employing quats and/or sulfonates (**5** or **6**) on the indocyanine backbone. Vilsmeier–Haack reagent **7** was synthesized and used for the condensation reaction with prepared intermediate indolium salts in anhydrous sodium acetate. Finally, to permit subsequent conjugation of targeting ligands and biomolecules, a bifunctional phenoxypropionic acid linkage was introduced on the *meso*-chlorine atom. Using microwave synthesis, we were able to achieve an extremely high conversion ratio (> 98%) and yield (> 85%) of the final reaction (Table S1). The crude product was washed with diethyl ether three times and was precipitated with methanol and diethyl ether (20 mL, 1:4) to give the final compounds **10** (ZW800-1) and **11** (ZW800-3a) as a dark green solid. Chemical purity of ZW800-1 and

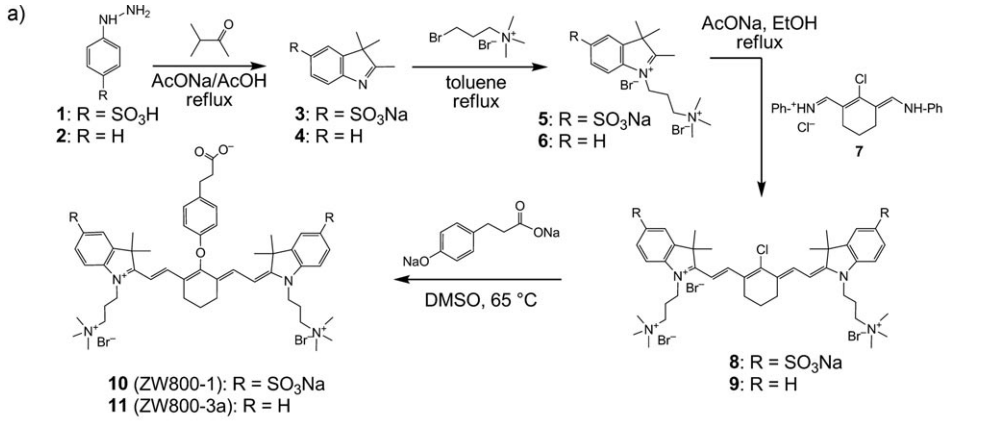

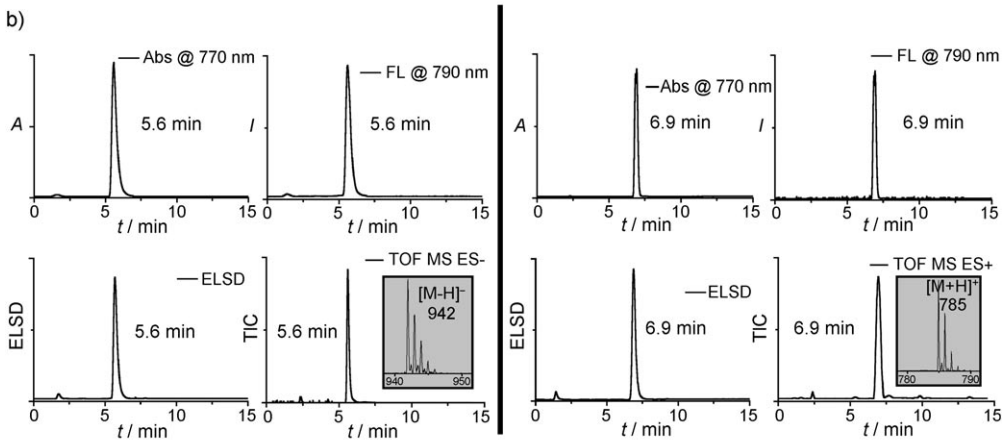

Compound	Formula	Calcd. [%]	Found [%]
10 (ZW800-1)	$C_{51}H_{66}Br_2N_4Na_2O_9S_2 \cdot 4\,H_2O$	C 50.16; H 6.11; N 4.59	C 49.88; H 6.23; N 4.26
11 (ZW800-3a)	$C_{51}H_{68}Br_2N_4O_3 \cdot 4\,H_2O$	C 60.23; H 7.53; N 5.51	C 59.73; H 7.56; N 5.40

Figure 1. Synthesis and characterization of 800 nm zwitterionic heptamethine indocyanine NIR fluorophores (ZW dyes). a) Synthetic scheme for zwitterionic heptamethine indocyanine NIR fluorophores. b) LC–MS and elemental analysis: absorbance at 770 nm (top left), fluorescence ($\lambda_{ex} = 770$ nm and $\lambda_{em} = 790$ nm; top right), ELSD (bottom left), and total ion chromatogram (TIC; bottom right). Insert: ESI-TOF mass spectrum of 5.6 min peak for ZW800-1 and 6.9 min peak for ZW800-3a.

ZW800-3a was 97.1% and 98.7%, respectively (Figure 1b). The ^{1}H NMR spectrum, the ^{13}C NMR spectrum, and ESI-TOF MS were consistent with the proposed structures (Figure S1–S2). Owing to the polar and hygroscopic nature of the final compounds, both ZW800-1 and ZW800-3a included four extra water molecules, as was analyzed by CHN elemental analysis (see the Supporting Information for details).

The hypothesis guiding our work was that zwitterionic small molecules might recapitulate the results seen previously with nanoparticles, namely lower in vivo background fluorescence. To test this hypothesis, we analyzed a series of heptamethine indocyanine NIR fluorophores that systematically varied in net charge as follows: −4 (CW800), −2 (RS800), −1 (ICG), 0 (ZW800-1), and +2 (ZW800-3a). The chemical structures and energy-minimized 3D structures of these NIR fluorophores are shown in Figure 2a. A note should be made of the significantly different distributions of charge and hydrophobicity over the surface of each molecule. The physicochemical and optical properties of these fluorophores are detailed in Table 1, Figure 2b, S3–S4. Although net charge and log$D$ at pH 7.4 varied widely, most optical parameters were similar and all compounds were stable (> 94%) in warm serum for up to 4 h.

Serum protein binding was measured by gel filtration chromatography (GFC) after incubation in 100% serum (Figure S5). ICG, which is known to bind serum proteins such as α_1-lipoprotein, γ-globulin, and serum albumin,[4,20] showed a significant HD shift after 4 h of incubation in FBS due to its hydrophobic character (log$D$ = 7.88) and net negative charge (+1/−2, net charge = −1). However, ZW800-1, with high hydrophilicity (log$D$ = −3.56) and balanced, alternating charge (+3/−3, net charge = 0) distributed evenly over its surface, did not adsorb to serum proteins. Although its log$D$ value at pH 7.4 is extremely low (−6.95), ZW800-3a showed low levels of protein adsorption when exposed to 100% serum, which is likely due to its unbalanced charge distribution (+3/−1, net charge = +2).

To investigate the effect of chemical structure and net charge on in vivo biodistribution and clearance, the NIR

Table 1: Comparison of chemical and optical properties of variously charged NIR fluorophores in 100% FBS.[a]

Property	CW800	RS800	ICG	ZW800-1	ZW800-3a
MW [Da]	1091	887	775	1149	945
net Charge	−4	−2	−1	0	+2
log$D$ at pH 7.4	2.51	0.11	7.88	−3.56	−6.95
ε [$M^{-1}cm^{-1}$]	237000	240000	121000	249000	309000
λ_{exc} [nm]	786	784	807	772	774
λ_{em} [nm]	800	800	822	788	790
Stokes shift [nm]	14	16	15	16	16
Φ [%]	14.2	16.9	9.3	15.1	16.1
decomposition [%]	4.0	4.4	5.9	5.5	3.8

[a] CW800: IRDye800-CW carboxylic acid; ICG: indocyanine green; RS800: IRDye800-RS carboxylic acid; ZW: zwitterionic.

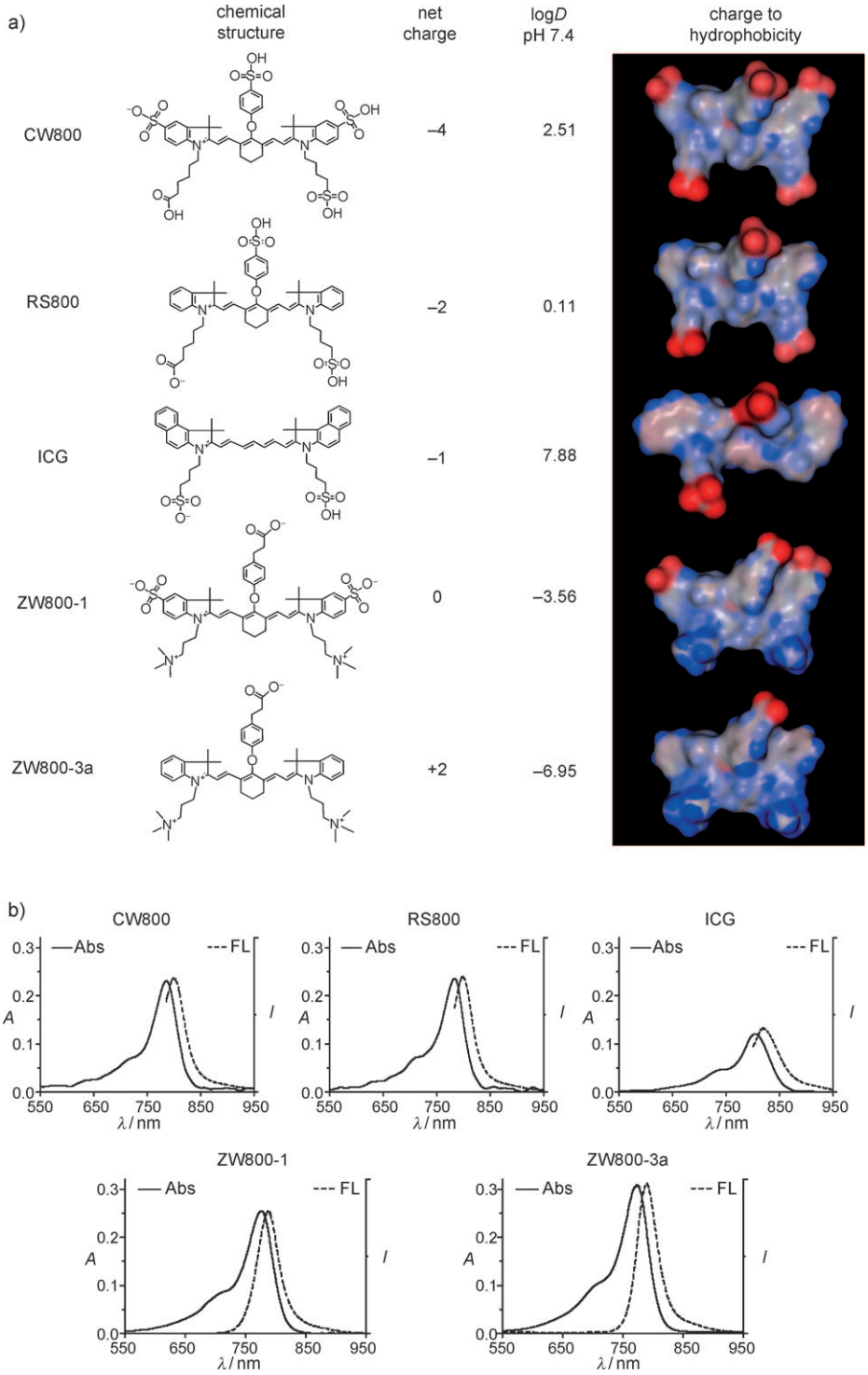

Figure 2. Physicochemical and optical properties of NIR fluorophores having systematically varying net charge. a) All molecules shown are bifunctional, permitting conjugation through their single carboxylic acid group, except ICG. Red: negative charge; blue: positive charge; gray: hydrophobicity. b) Absorbance and fluorescence emission spectra of each fluorophore in 100% FBS (1 μM) supplemented with 50 mM HEPES, pH 7.4.

fluorophore series was injected intravenously into mice and rats. Using the fluorescence-assisted resection and exploration (FLARE) intraoperative image-guided surgery system,[21,22] we measured the behavior of injected fluorophores in real time over 4 h. As shown in Figure 3a, the β phase blood half-life ($t_{1/2\beta}$) of CW800 (−4), RS800 (−2), ICG (−1), ZW800-1 (0), and ZW800-3a (+2) in CD-1 mice was 18.5, 11.2, 3.6, 15.1, and 28.1 min, respectively. All half-life values were statistically different from each other by analysis of variance (ANOVA). Elimination of NIR fluorophores from the body by renal clearance also varied markedly (Table 2), with ICG being undetectable in urine (caused by liver uptake and subsequent biliary clearance) and ZW800-1 being mostly renally cleared. The fraction of the injected dose that was eliminated from the body into urine by 4 h postinjection in mice was 44.0 ± 4.6 %ID, 15.5 ± 1.2 %ID, 2.2 ± 0.9 %ID, 86.0 ± 15.4 %ID, and 23.2 ± 11.4 %ID, respectively for CW800 (−4), RS800 (−2), ICG (−1), ZW800-1 (0), and ZW800-3a (+2; see also Figure S6–S8). In fact, only 1 h after injection, 51.3 ± 9.7 %ID of ZW800-1 was found in urine.

Uptake of NIR fluorophores in organs and tissues of mice and rats also varied markedly. As shown in Figure 3b (see also Figure S6–S8 and Videos S1–S3), all anionic and cationic NIR fluorophores exhibited high nonspecific uptake in a variety of organs, with anionic NIR fluorophores exhibiting significant excretion into bile, resulting in high NIR fluorescent signal throughout the GI tract. For example, at 4 h postinjection, uptake values for CW800 (−4) were: intestine: 28.5 ± 7.0 %ID/g, liver: 11.4 ± 0.8 %ID/g, and kidneys: 7.3 ± 1.3 %ID/g. For ICG (−1), uptake values were: intestine: 62.0 ± 6.6 %ID/g, liver: 27.1 ± 0.5 %ID/g, and kidneys: 5.9 ± 1.0 %ID/g, which were also caused by the extremely high hydrophobicity/lipophilicity of ICG (log*D* at pH 7.4 = 7.88). Two positive charges of ZW800-3a (+2) resulted in unfavorable biodistribution, mostly found in the liver (40.6 ± 2.6 %ID/g), intestine (11.5 ± 3.4 %ID/g), and kidneys (9.0 ± 1.1 %ID/g). On the contrary, ZW800-1 was exclusively cleared by the kidneys, with no appreciable

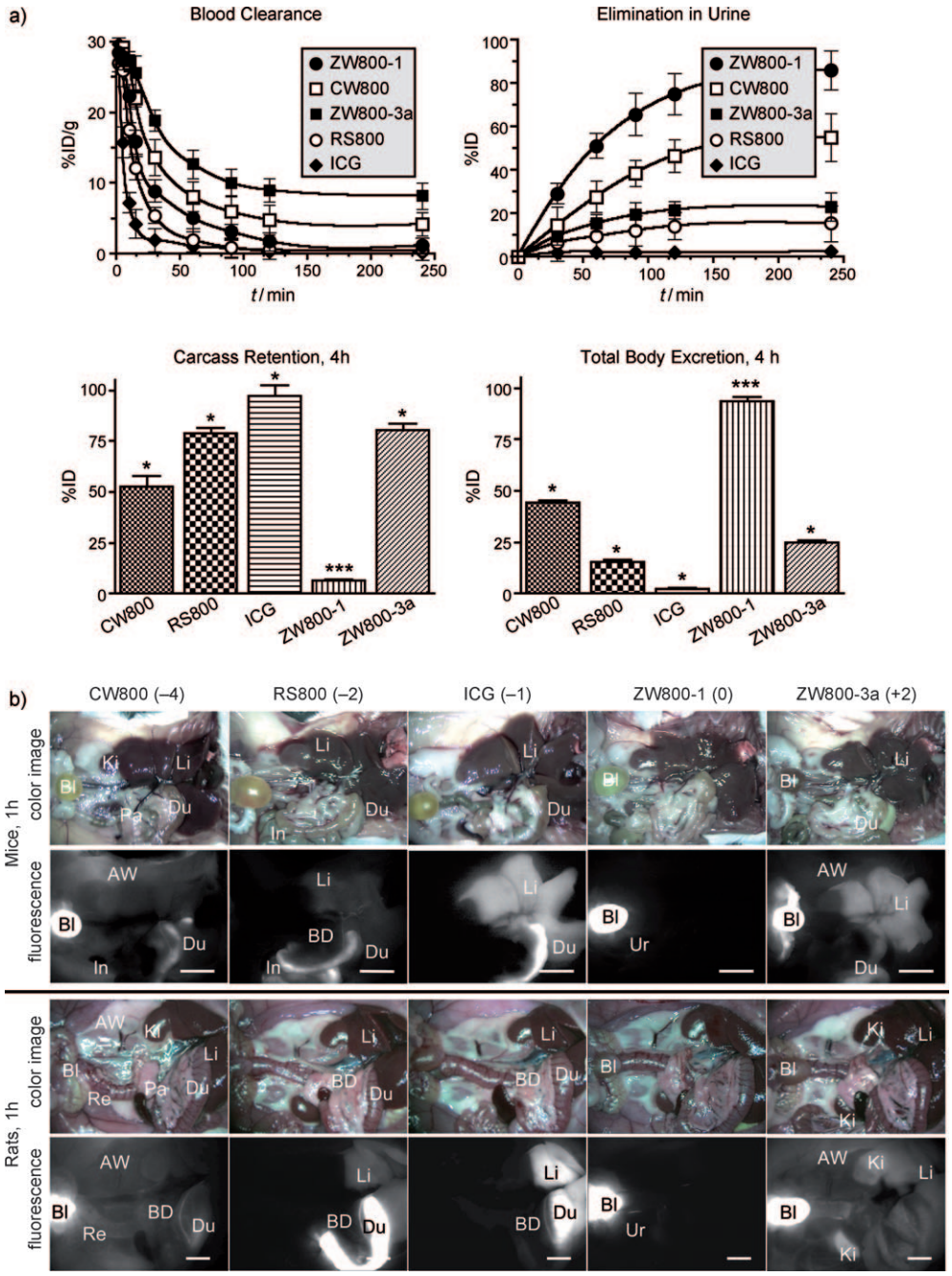

Figure 3. Biodistribution and clearance of NIR fluorophores. a) Blood concentration (%ID/g), elimination in urine (%ID), carcass retention (%ID), and total body clearance (%ID) in CD-1 mice. Each data point is the mean ± S.D. from $N = 5$ animals. $^{*}P < 0.01$ and $^{***}P < 0.001$ for pairwise comparisons of half-life using ANOVA. b) NIR fluorophores (40 pmol g^{-1}) were injected intravenously into CD-1 mice (top two panels) and SD rats (bottom two panels), 1 h prior to imaging. Shown are color and 800 nm NIR fluorescence images of surgically exposed organs/tissues. Abbreviations used are: AW: abdominal wall; Bl: bladder; BD: bile duct; Du: duodenum; In: intestine; Ki: kidneys; Li: liver; Lu: lungs; Pa: pancreas; Re: rectum; Sk: skin; Ur: ureter. Scale bars: 1 cm.

nonspecific background signal in any tissues and organs and only 12.4 ± 3.4 %ID remaining in the carcass at 4 h post-injection, mostly in the kidneys (9.8 ± 2.2 %ID/g) and only negligible amounts in the liver (0.9 ± 0.1 %ID/g) and intestine (0.7 ± 0.4 %ID/g). Similar results were observed in rats, but excretion rates were slightly slower than those in mice (Table 2). It should be emphasized that no single value, such as log*D* or net charge, is predictive of in vivo fate. Optimal in vivo behavior appears to be mediated by alternating and balanced charge, distributed over the entire surface of the molecule, which completely shields the underlying hydrophobicity.

The most common strategy to engineer targeted NIR fluorescent contrast agents is to employ "modular" chemistry,[23–25] which covalently combines an NIR fluorophore and a high-affinity, small-molecule-targeting ligand. However, commercially available NIR fluorophores are typically hydrophobic and/or di-/tetra-sulfonated. One of the key results of our study is that purely anionic or cationic NIR fluorophores exhibit significant nonspecific uptake in normal tissues and organs, although their log*D* at 7.4 is extremely low (i.e., hydrophilic). For molecules that have a high "hydrophobic moment" like ICG, liver uptake was significant and rapid, thus reducing blood concentration, but increasing NIR fluorescence of the liver, bile, and GI tract.[26] This rapid uptake contaminates the liver and/or lower GI tract with high signal and precludes many important image-guided surgeries of the abdomen. The blood half-life of ICG was only 2 to 5 min because of the rapid liver uptake. RS800 had a lower hydrophobic moment, but still had exposed aromatic groups that were recognized by the liver and resulted in rapid excretion into bile (short transit time through the liver). However, it also had enough charge to keep it in the bloodstream long enough to undergo approximately 20 % renal filtration. For highly anionic CW800, the hydrophobic moment was compensated by the charge (more hydrophilic)

Table 2: In vivo organ/tissue distribution of variously charged NIR fluorophores 4 h postinjection into mice ($N=5$) and rats ($N=5$).[a]

Fluorophore	Species	Ki	Sk/Mu	He/Lu	Sp	Li	In	Re	Bl	Carcass	Eliminated
CW800	mouse	+	+	−	−	−	+++	++	+++	52.4 ± 9.6 %ID	44.0 ± 4.6 %ID
	rat	++	+	−	−	+	+++	+	+++	N.D.	N.D.
RS800	mouse	+	−	−	−	−	++	+++	++	79.0 ± 4.1 %ID	15.5 ± 1.2 %ID
	rat	+	−	−	−	−	+++	++	−	N.D.	N.D.
ICG	mouse	−	−	−	−	++	+++	+	−	97.1 ± 9.4 %ID	2.2 ± 0.9 %ID
	rat	−	−	−	−	++	+++	+	−	N.D.	N.D.
ZW800-1	mouse	−	−	−	−	−	−	−	+++	12.4 ± 3.4 %ID	86.0 ± 15.4 %ID
	rat	+	−	−	−	−	−	−	+++	14.8 ± 6.5 %ID	83.4 ± 15.9 %ID
ZW800-3a	mouse	+	+	−	−	++	+++	+	+++	68.6 ± 8.6 %ID	23.2 ± 11.4 %ID
	rat	++	++	+	+	+++	++	−	+++	68.3 ± 15.7 %ID	28.7 ± 16.3 %ID

[a] Abbreviations used are: Bl: bladder; He: heart; In: intestine; Ki: kidneys; Li: liver; Lu: lungs; Mu: muscle; Re: rectum; Sk: skin; Sp: spleen; and N.D.: not done. All mouse values were measured directly. Shown for each measurement is mean ± S.D. The CBR of each organ/tissue relative to the abdominal wall was quantified and labeled as −: 0 to 1; +: 1 to 2; ++: 2 to 5; and +++: > 5.

that resulted in approximately 55 % renal filtration,[27] but also significant liver clearance,[28] GI tract contamination, and nonspecific uptake in normal tissues and organs. The high cationic charge of ZW800-3a caused the molecule to exhibit high nonspecific uptake in almost every tissue and organ in the body, thus resulting in only approximately 20 % renal excretion. Only a true zwitterionic molecule, such as ZW800-1, with charge balanced over the entire surface and hydrophobicity well shielded by this charge, does not exhibit protein binding, nonspecific tissue/organ uptake, or liver clearance. Although the precise mechanism for this observation is not yet known, zwitterionic molecules likely minimize the interaction with serum proteins by charge shielding,[29] and minimize penetration of cellular membranes by extreme polarity.[30,31]

As our efforts focused on lowering of the background fluorescence, it would have been counter-productive if this lowering were achieved at the expense of the signal. This issue is a major problem, for example, when utilizing two-photon upconversion strategies for NIR fluorescence. Fortunately, we demonstrate that the optical properties of zwitterionic NIR fluorophores are excellent. In fact, the product of the extinction coefficient and quantum yield of ZW800-1 in serum are more than three times higher than that of the FDA-approved NIR fluorophore ICG (Table 1). In addition, the 800 nm zwitterionic heptamethine indocyanine NIR fluorophore ZW800-1 has remarkable in vivo properties, including no serum protein binding, rapid renal clearance, and ultralow nonspecific tissue uptake (i.e., background). ZW800-1 also provides a single carboxylic acid for the covalent conjugation to targeting ligands through a stable amide bond; because of these features, ZW800-1 has been selected by the US National Cancer Institute's Experimental Therapeutics (NExT) Program as a first-in-class molecule for rapid translation into human clinical studies.

A key unanswered question in the present study is whether a targeted NIR fluorophore made zwitterionic by choosing the proper ZW800 ± *i* fluorophore for conjugation requires intermingled positive and negative charges over the entire surface of the final molecule (similar to unconjugated ZW800-1), or whether a dipole-like zwitterionic structure is adequate for improved in vivo performance. Ongoing studies are also focused on the engineering of a family of 700 nm zwitterionic NIR fluorophores to complement those we now have at 800 nm. When used with the two NIR channel capabilities of the FLARE imaging system, it should be possible to simultaneously image two independent targeted NIR fluorophores during surgery. This approach is especially important in cancer surgery when resection of the tumor (i.e., using one NIR channel) needs to be performed, while avoiding critical structures such as vessels and nerves (i.e., using the second NIR channel).

Experimental Section

Synthesis of ZW800–1 (**10**) and ZW800–3a (**11**). As depicted in Figure 1 a, starting materials **1**–**4** were used to prepare the 800 nm emitting, zwitterionic heptamethine indocyanine fluorophores **10** (ZW800-1) and **11** (ZW800-3a). All products **5**–**11** were obtained in reasonably high purity as indicated by TLC analyses by using C18 adsorbents and high-resolution ^{1}H and ^{13}C nuclear magnetic resonance (NMR) spectra. Chemical purity was measured by using HPLC combined with simultaneous evaporative light scatter detection (ELSD), absorbance (photodiode array), fluorescence, and ESI-TOF MS. Compounds were also analyzed by MALDI-TOF MS and CHN elemental analysis. See Supporting Information for detailed chemical syntheses and analyses.

Optical and physicochemical property analyses: Commercially available NIR fluorophores included IRDye 800-CW (CW800; Li-Cor, Lincoln, NE), IRDye 800-RS (RS800; Li-Cor), and indocyanine green (ICG; Akorn, Decatur, IL). When only an *N*-hydroxysuccinimide (NHS) ester was available, the corresponding carboxylic acid (CA) was formed by incubation at high concentration in borate buffer (50 mM), pH 9.0 for 3 h followed by dilution into the desired buffer. All optical measurements were performed at 37 °C in phosphate-buffered saline (PBS), pH 7.4 or 100 % fetal bovine serum (FBS) buffered with HEPES (50 mM, pH 7.4). For fluorescence quantum yield (Φ) measurements, ICG in dimethyl sulfoxide ($\Phi = 13\,\%$) was used as a calibration standard under conditions of matched absorbance at 770 nm.[14–19] For in vitro optical property measurements, online fiberoptic HR2000 absorbance (200–1100 nm) and USB2000FL fluorescence (350–1000 nm) spectrometers (Ocean Optics, Dunedin, FL) were used. NIR excitation was provided by a 770 nm NIR laser diode light source (Electro Optical Components, Santa Rosa, CA) set to 8 mW and coupled through a 300 μm core diameter, NA 0.22 fiber (Fiberguide Industries, Stirling, NJ). In silico investigations of the partition coefficient (log*D*) and surface molecular charge and hydrophobicity were carried out using MarvinSketch 5.2.1 (ChemAxon, Budapest, Hungary).

In vivo biodistribution and clearance: Animals were housed in an AAALAC-certified facility and were studied under the supervision of an approved institutional protocol. CD-1 male mice weighing 25 to 30 g and Sprague-Dawley (SD) male rats weighing 250 to 300 g were purchased from Charles River Laboratories (Wilmington, MA). 40 pmol g^{-1} of NIR fluorophores in saline were administered intravenously, and animals were imaged with the FLARE real-time intraoperative imaging system as described in detail previously.[21] For fluorescence excitation, 14 mW cm^{-2} of 745 to 779 nm-filtered light was used, and for emission, light was filtered using a 800 to 848 nm bandpass filter. For each experiment, camera exposure time and image normalization was held constant. Color video images were collected on a separate channel using custom-designed optics and software. To quantify the blood clearance rate and urinary excretion, intermittent sampling from the tail vein was performed over 4 h. Approximately 20 μL of blood and urine were collected at the following time points using glass capillary tubes: 0, 1, 2, 5, 10, 15, 30, 60, 90, 120, 180, and 240 min. The FLARE imaging system measured the fluorescence intensity of each sample, and the concentration was calculated based on CBR (defined below) using a standard curve for each fluorophore. To measure total body excretion in mice, animals were sacrificed at 30, 60, 90, 120, 180, and 240 min, and major tissues and organs were resected, lyophilized, weighed, and re-dissolved in tissue lysate buffer. The tissue-containing solutions were homogenized using a bullet blender (Next Advance, Averill Park, NY). Using capillary tubes, the amount of NIR fluorophore in each organ/tissue was quantified by measuring fluorescent intensity (CBR), which was converted to concentration (%ID/g) or amount (%ID) based on organ/tissue weight.

Quantitative analysis: At each time point, the fluorescence (FL) and background (BG) intensity of a region of interest (ROI) over each organ/tissue was quantified using custom FLARE software. The contrast-to-background ratio (CBR) was calculated as CBR = (FL-BG)/BG. At least 3 animals were analyzed at each time point. Statistical analysis was carried out using the unpaired Student's *t* test or one-way analysis of variance (ANOVA). Results were presented as mean ± S.D. and curve fitting was performed using Prism version 4.0a software (GraphPad, San Diego, CA).

Received: April 8, 2011
Published online: June 7, 2011

Keywords: biodistribution · clearance · fluorescent probes · imaging agents · near-infrared fluorophores

[1] J. V. Frangioni, *Curr. Opin. Chem. Biol.* **2003**, *7*, 626 – 634.
[2] H. Kobayashi, M. Ogawa, R. Alford, P. L. Choyke, Y. Urano, *Chem. Rev.* **2009**, *109*, 5288.
[3] S. Achilefu, *Angew. Chem.* **2010**, *122*, 10010 – 10012; *Angew. Chem. Int. Ed.* **2010**, *49*, 9816 – 9818.
[4] S. Ohnishi, S. J. Lomnes, R. G. Laurence, A. Gogbashian, G. Mariani, J. V. Frangioni, *Mol. Imaging* **2005**, *4*, 172 – 181.
[5] H. Lee, J. C. Mason, S. Achilefu, *J. Org. Chem.* **2006**, *71*, 7862 – 7865.
[6] L. Strekowski, M. Lipowska, G. Patonay, *J. Org. Chem.* **1992**, *57*, 4578 – 4580.
[7] G. Patonay, J. Salon, J. Sowell, L. Strekowski, *Molecules* **2004**, *9*, 40 – 49.
[8] Z. Zhang, K. Liang, S. Bloch, M. Berezin, S. Achilefu, *Bioconjugate Chem.* **2005**, *16*, 1232 – 1239.
[9] K. Kiyose, H. Kojima, Y. Urano, T. Nagano, *J. Am. Chem. Soc.* **2006**, *128*, 6548 – 6549.
[10] H. Kobayashi, Y. Koyama, T. Barrett, Y. Hama, C. A. Regino, I. S. Shin, B. S. Jang, N. Le, C. H. Paik, P. L. Choyke, Y. Urano, *ACS Nano* **2007**, *1*, 258 – 264.
[11] K. Chen, J. Xie, X. Chen, *Mol. Imaging* **2009**, *8*, 65 – 73.
[12] S. Lee, J. H. Ryu, K. Park, A. Lee, S. Y. Lee, I. C. Youn, C. H. Ahn, S. M. Yoon, S. J. Myung, D. H. Moon, X. Chen, K. Choi, I. C. Kwon, K. Kim, *Nano Lett.* **2009**, *9*, 4412 – 4416.
[13] S. A. Hilderbrand, R. Weissleder, *Curr. Opin. Chem. Biol.* **2010**, *14*, 71 – 79.
[14] H. S. Choi, W. Liu, P. Misra, E. Tanaka, J. P. Zimmer, B. Itty Ipe, M. G. Bawendi, J. V. Frangioni, *Nat. Biotechnol.* **2007**, *25*, 1165 – 1170.
[15] W. Liu, H. S. Choi, J. P. Zimmer, E. Tanaka, J. V. Frangioni, M. Bawendi, *J. Am. Chem. Soc.* **2007**, *129*, 14530 – 14531.
[16] H. S. Choi, B. I. Ipe, P. Misra, J. H. Lee, M. G. Bawendi, J. V. Frangioni, *Nano Lett.* **2009**, *9*, 2354 – 2359.
[17] H. S. Choi, W. Liu, F. Liu, K. Nasr, P. Misra, M. G. Bawendi, J. V. Frangioni, *Nat. Nanotechnol.* **2010**, *5*, 42 – 47.
[18] H. S. Choi, Y. Ashitate, J. H. Lee, S. H. Kim, A. Matsui, N. Insin, M. G. Bawendi, M. Semmler-Behnke, J. V. Frangioni, A. Tsuda, *Nat. Biotechnol.* **2010**, *28*, 1300 – 1303.
[19] H. S. Choi, J. V. Frangioni, *Mol. Imaging* **2010**, *9*, 291 – 310.
[20] R. J. Williams, M. Lipowska, G. Patonay, L. Strekowski, *Anal. Chem.* **1993**, *65*, 601 – 605.
[21] S. L. Troyan, V. Kianzad, S. L. Gibbs-Strauss, S. Gioux, A. Matsui, R. Oketokoun, L. Ngo, A. Khamene, F. Azar, J. V. Frangioni, *Ann. Surg. Oncol.* **2009**, *16*, 2943 – 2952.
[22] S. Gioux, H. S. Choi, J. V. Frangioni, *Mol. Imaging* **2010**, *9*, 237 – 255.
[23] V. Humblet, P. Misra, J. V. Frangioni, *Contrast Media Mol. Imaging* **2006**, *1*, 196 – 211.
[24] Y. Ye, S. Bloch, B. Xu, S. Achilefu, *Bioconjugate Chem.* **2008**, *19*, 225 – 234.
[25] H. Qian, Y. Gu, M. Wang, S. Achilefu, *J. Fluoresc.* **2009**, *19*, 277 – 284.
[26] A. Matsui, E. Tanaka, H. S. Choi, J. H. Winer, V. Kianzad, S. Gioux, R. G. Laurence, J. V. Frangioni, *Surgery* **2010**, *148*, 87 – 95.
[27] E. Tanaka, S. Ohnishi, R. G. Laurence, H. S. Choi, V. Humblet, J. V. Frangioni, *J. Urol.* **2007**, *178*, 2197 – 2202.
[28] E. Tanaka, H. S. Choi, V. Humblet, S. Ohnishi, R. G. Laurence, J. V. Frangioni, *Surgery* **2008**, *144*, 39 – 48.
[29] I. J. Colton, J. D. Carbeck, J. Rao, G. M. Whitesides, *Electrophoresis* **1998**, *19*, 367 – 382.
[30] L. Bourré, F. Giuntini, I. M. Eggleston, M. Wilson, A. J. MacRobert, *Br. J. Cancer* **2009**, *100*, 723 – 731.
[31] R. F. Zwaal, P. Comfurius, L. L. van Deenen, *Nature* **1977**, *268*, 358 – 360.

